GLOBAL SCIENCE LIBRARY

RESEARCH

Journal of Clinical & Medical Imaging

Accurate estimation of diffusion kurtosis (DK) imaging parameters of the prostate

Yousef Mazaheri[1,2*], Andreas M Hotker[2], Amita Shukla-Dave[1,2], Hedvig Hricak[2] and Oguz Akin[2]

[1]Department of Medical Physics, Memorial Sloan Kettering Cancer Center, New York, NY, USA

[2]Department of Radiology, Memorial Sloan Kettering Cancer Center, New York, NY, USA

Abstract

Purpose: *To evaluate the performance of maximum likelihood (ML) estimation of diffusion kurtosis (DK) imaging parameters in the prostate and compare the estimated parameters to those measured using least squares (LS) estimation.*

Materials and methods: *The institutional review board issued a waiver of informed consent for this Health Insurance Portability and Accountability Act (HIPAA)-compliant, retrospective study of forty-two patients (median [Md] age=61 years; range: 43-74 years) who underwent magnetic resonance imaging (MRI) between September and October 2016. Diffusion-weighted MRI (DW-MRI) at nine b-values (0-2000 s/mm^2) were acquired using a 3-T whole-body MRI unit (Discovery MR750; GE Medical Systems, Waukesha, WI) equipped with an eight-channel phased array coil for signal reception. Diffusion coefficient (D) and kurtosis (K) were estimated from the normal appearing prostate peripheral zone and prostate cancer regions of interest (ROIs). The parameters were estimated by fitting the measured MR signal intensities as a function of b-value, using LS and ML algorithms. An estimate of the noise was obtained on the b=0 images in an artifact-free ROI in the rectum. Simulations were also carried out to assess the properties of the two estimators in a range of signal-to-noise ratios.*

Results: *For benign ROIs, the mean D ± standard deviation, (1.88±0.52)×10^{-3} mm^2/sec, and mean K (0.79±0.20), measured using LS estimation, differed significantly from the mean D (1.96±0.48)×10^{-3} mm^2/sec and mean K (0.68±0.21), measured using ML estimation (P<0.001 for both). For malignant ROIs, the mean D (1.48±0.38)×10^{-3} mm^2/sec and mean K (0.94±0.20), measured using LS estimation, differed significantly from the mean D (1.54±0.36)×10^{-3} mm^2/sec and mean K (0.81±0.19), measured using ML estimation (P<0.001 for both). Simulations demonstrate that ML minimizes the bias estimate of DK parameters within the signal-to-noise ratio range of 5-15.*

Conclusion: *By incorporating the noise level, the ML estimation increases the accuracy of DK parameter estimation. In vivo results with phased array coils showed significant differences in DK parameter estimates with ML as compared with the standard LS estimation.*

Keywords: *diffusion-weighted MRI, diffusion kurtosis imaging, prostate, signal-to-noise ratio, least squares, maximum likelihood*

Introduction

In biological tissues, microscopic motion, which is detected by diffusion-weighted magnetic resonance imaging (DW-MRI), includes both diffusion of water molecules (influenced by the structural components of the tissue) and complex underlying cellular components and structures that hinder and restrict the diffusion of water molecules. Diffusion kurtosis (DK) has been proposed as a metric for quantifying the behavior of water diffusion, in a restricted environment, to provide an indication of tissue microstructure [1]. In an unrestricted environment, water diffuses essentially at random, and the probability distribution of water diffusion has a Gaussian shape. However, in human tissue- and particularly in tumors, where cells are more densely packed- water diffusion is restricted by interactions with cell membranes and other microstructural components. DK measures the deviation of the diffusion displacement profile from a Gaussian distribution, and hence, enables the impact of complex structures on water diffusion [1-3].

To fit parameters to the measured MR signal intensities as a function of b-value, a non-linear least squares (LS) algorithm is usually used, which assumes that the noise is normally distributed. Noise in magnitude MR images follows a Rice distribution, which tends toward a normal distribution at higher signal-to-noise ratios (SNRs), but at high b-values the Gaussian assumption can lead to significant error in diffusion parameter estimation [4]. The Rician noise, at low SNR images and high b-values, can be incorporated into a maximum likelihood (ML) optimization to provide unbiased diffusion parameter estimates [4,5]. If an appropriate noise model is available, the ML can generate unbiased parameter estimates and has the ability to estimate parameter uncertainties. For example, in a study of tumors using apparent diffusion coefficient (ADC), Walker-Samuel, et al. showed that ML reduces the bias (underestimation) in ADC estimation [6].

DK has been evaluated by several groups in the prostate [7-11]. To our knowledge there has been no report to address the bias associated with estimation of DK parameters at low SNR. Therefore, the purpose of the present study is to investigate the influence of noise on DK parameters in the prostate and evaluate ML as a means to provide more accurate estimates of DK parameters.

Materials and methods

Simulations

Monte Carlo simulation was carried out to assess the properties of the two fitting algorithms at a range of SNRs (range: 5-25). Data were simulated by adding Gaussian noise to complex signal (real and imaginary components) for an eight-channel (*N*rec=8) phased array coil, assuming uncorrelated noise, to simulate a Rician distribution of the magnitude signal [12]. The Monte Carlo sample size was 10, 000 and nine *b*-values were: 0, 400, 800, 1000, 1200, 1400, 1600, 1800, and 2000 sec/mm^2. The resultant signals were fitted to the DK model (see Supplementary Data). Sample mean and standard deviation (SD) for the estimators were calculated. All simulations were implemented in MATLAB™ software (R2014b, Mathworks, Natick, MA). Gaussian noise with zero mean and SD σ was added to both real and imaginary signal components in each channel. The performance of each estimator was evaluated in terms of its accuracy quantified using a bias estimate, which is defined as the difference between the expectation value of the estimator and the true value of the model parameter.

MRI data acquisition

The institutional review board waived the requirement for informed consent for this Health Insurance Portability and Accountability Act (HIPAA)-compliant, retrospective study. Between September 2016 and October 2016, forty-two patients (age: 43-74 years) with biopsy-proven prostate cancer (PCa) referred for MRI of the prostate underwent a pretreatment clinical MRI examination that included DW-MRI. MR imaging was performed with a 3-T whole-body MRI unit (Discovery MR750; GE Medical Systems, Waukesha, WI) equipped with an eight-channel phased array coil for signal reception.

DW-MR images were obtained using a spin-echo echo-planar imaging sequence with ramp sampling by using a pair of rectangular gradient pulses along with three orthogonal axes (repetition time msec/effective echo time msec, 4000/59.5–82.8 [Md 80 msec]; field of view, 16-24 cm; section thickness, 4 mm; no intersection gap). Nine *b*-values identical to the simulations between 0 and 2000 sec/mm^2 were acquired.

Image analysis

TA radiologist with knowledge of the location of cancerous sextants at biopsy traced suspected tumor areas and the normal-appearing peripheral zone (PZ) (i.e., regions of interest [ROIs]) using ImageJ software (U.S. National Institutes of Health). An additional ROI was placed within the air cavity inside the rectum where no apparent ghosting artifacts were present.

Images were post-processed off-line using code written in MATLAB™ software. *D* and K maps were calculated on a pixel-by-pixel basis using both the LS and ML. The ML requires an estimate of the Rician noise SD. A number of methods have been suggested in the literature to estimate σ [16,13-16]. Here, σ was measured similar to Andre´ for *N*rec coils (16) for *N*voxels voxels is based on the expression from [17] in terms of the signal for each voxel S_i:

$$\sigma = \sqrt{\frac{\sum_{i=1}^{Nvoxels} S_i^2}{2Nvoxels \cdot Nrec}} \quad [1]$$

Statistical analysis

All statistic analyses were performed using Matlab. The Wilcoxon signed rank test was used for pairwise comparisons. A P value less than 0.05 was considered to indicate a statistically significant difference.

Results

Simulations

Figure 1 shows an example of a simulated diffusion signal intensity curve fitted to the DK model using the LS and ML estimators in the normal PZ tissue with multiple b-value acquisitions. The measured signal at this SNR level (SNR=10) deviated from the true signal (no added noise, infinite SNR), which demonstrates the inherent bias present in the LS estimate of the DK parameters compared with the ML estimate.

In Figure 2, the different estimators are compared for mean DK parameters from benign PZ and PCa (obtained from Table 1) based on Monte Carlo simulations for Nrec=8 for a SNR range of 5-25. The ML estimator performs best in terms of bias, particularly at the lower SNR range of 5-15. LS underestimated *D* and overestimated *K* at this SNR range. At any given SNR, the bias associated with PZ parameters with LS estimation is larger than those of PCa.

Human results

Comparison of DK-derived parameters (Md and SD) in PZ and PCa ROIs from LS and ML algorithms are shown in the box-and-whisker plots of Figure 3 (Table 2). In PZ, the mean D values were 6.26% lower for the LS estimate as compared with the ML estimate. Mean K values were 22.51% higher for the LS estimate as compared with the ML estimate. In PCa, mean *D* values were 4.60% lower for the LS estimate as compared with the ML estimate. Mean *K* values were 18.55% higher for the LS estimate as compared with the ML estimate.

Figures 4 and 5 shows representative spatial maps of the DK parameters from the LS and ML algorithms of a slice that contains tumor. The dynamic range was the same for maps generated using LS and ML. The figure demonstrates the underestimation of *D* and overestimation of *K* by the LS algorithm in comparison with the ML algorithm. The scatter plots are the measured parameters (*D* and *K*) from voxels outlined in the prostate slice.

In Figure 6, examples of the maps from only the tumor regions are shown along with histograms of the distribution of DK parameters estimated from LS and ML algorithms. Of note is the shift in mean values for the distributions but also the larger width of the distribution measured by its SD.

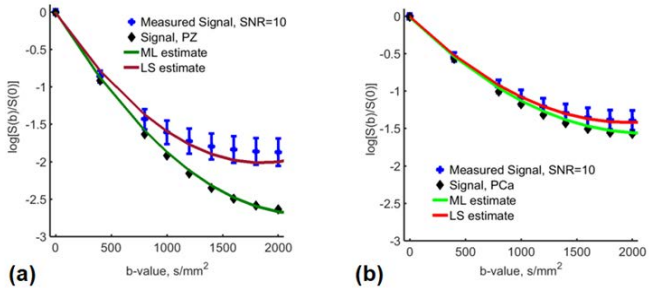

Figure 1. *Simulated decay curves of (A) prostate peripheral zone (PZ) and (B) prostate cancer (PCa) data. For the simulation, the signal-to-noise ratio (SNR) was 10 and Nrec=8 channels. The data were fitted to the model using the least squares (LS) and maximum likelihood (ML) estimators. The 'true' diffusion coefficient (D) of PZ is D(PZ)=2.51×10-3 mm2/s and of PCa is D(PCa)=1.55×10-3 mm2/s. The 'true' kurtosis (K) of PZ is K(PZ)=0.57 and of PCa is K(PCa)=0.96 based on values reported in Reference [7].*

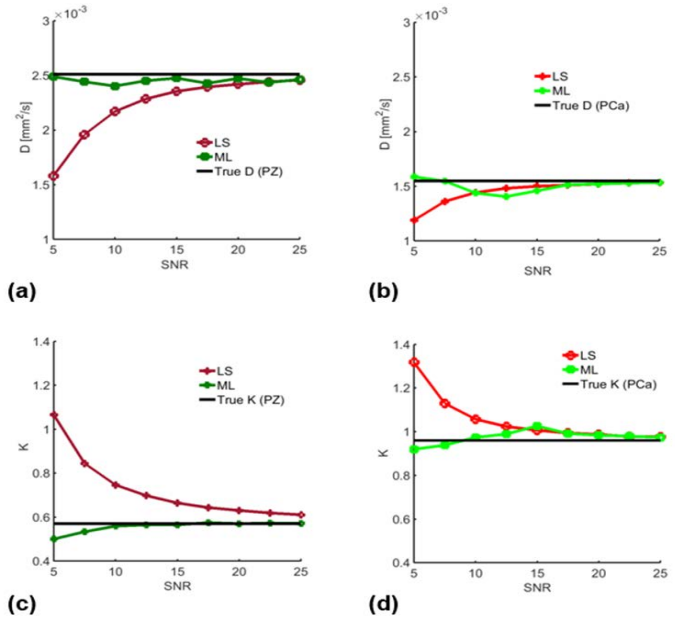

Figure 2. *Monte Carlo simulation results for eight-channel (Nrec=8) phased array coil obtained from signal-to-noise (SNR) range 5-25. (A and B) Averaged diffusion coefficient (D) values of peripheral zone (PZ) and prostate cancer (PCa) from simulation sample size of 10 000. (C and D) Averaged kurtosis (K) values of PZ and PCa. True D and K values were obtained from Reference [7].*

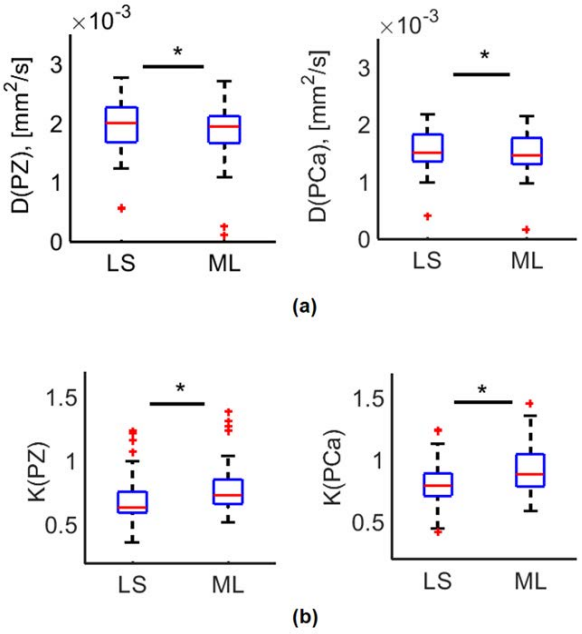

Figure 3. *Box-and-whisker plots of (a) median D (mm2/s) and (b) median K in PCa and benign PZ ROIs from 42 patients estimated from LS and ML. Red lines median values; bottom of box, 25 percentiles; top of box, 75th percentile. The Wilcoxon signed rank test demonstrated statistical significance for differences between DK parameters between the two estimates for D and K.*

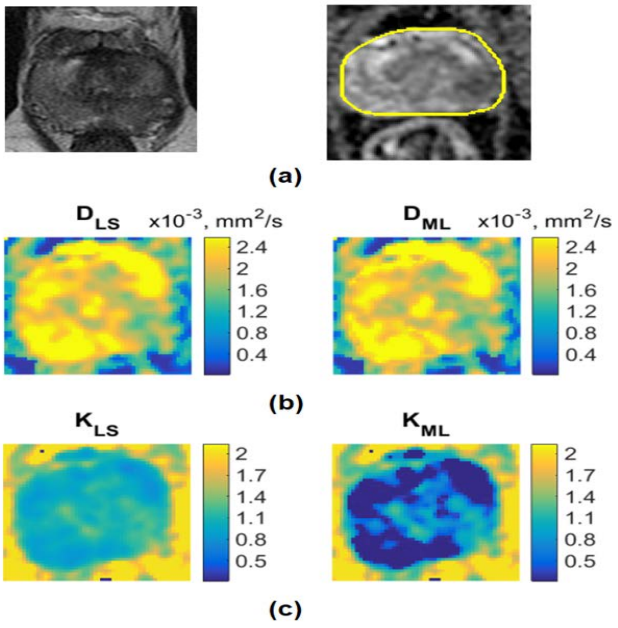

Figure 4. (A) Transverse T2-weighted image and ADC map of the prostate from a 51-year-old patient with tumor located in the PZ (presurgical PSA level, 4.5 ng/mL; biopsy Gleason score, 8 [4+4]). Maps of (B) D, and (C) K obtained using LS and ML curve fitting. For D, the color bar is in the units of mm²/s: min-max: 0.2-2.4×10-3 mm²/s; for K, min-max: 0.2-2.

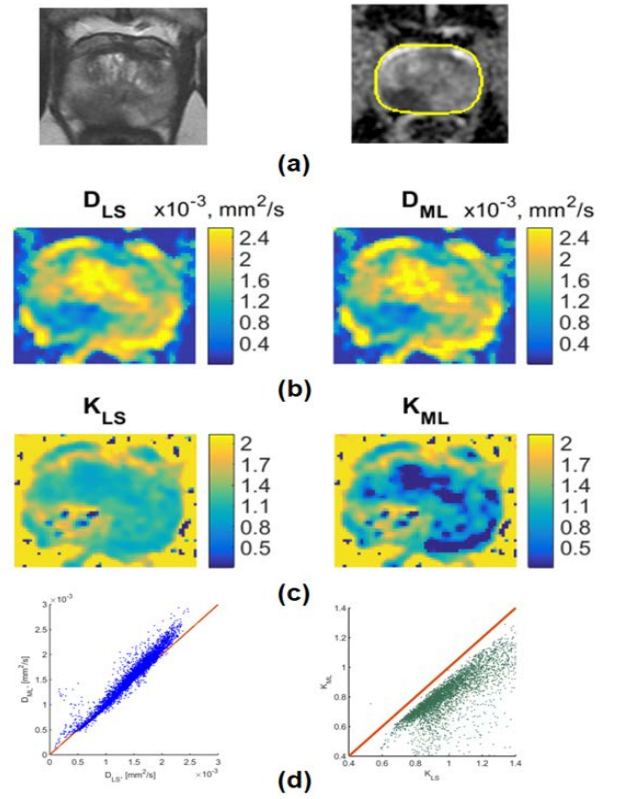

Figure 5: (A) Transverse T2-weighted image and ADC map of the prostate from a 64-year-old patient with tumor located in the PZ (presurgical PSA level, 12.8 ng/mL; biopsy Gleason score, 7 [3+4]). Maps of (B) D, and (C) K obtained using LS and ML curve fitting. For D, the color bar is in the units of mm2/s: min-max: 0.2-2.4×10-3 mm2/s; for K, min-max: 0.2-2. (D) Scatter plot of D and K. ML provides higher estimates of D and lower estimates of K as compared with the standard LS estimation. The bias associated with PZ parameters with LS estimation is larger than those of PCa.

	D [×10-3mm²/s]	K
Benign PZ	2.51 ± 0.37	0.57 ± 0.07
Cancerous sextant	1.55 ± 0.45	0.96 ± 0.24

Table 1. *Mean ± standard deviations values of benign peripheral zone (PZ) and cancerous sextant reported in Reference [7].*

	Peripheral zone			**Prostate cancer**		
	LS	ML	P value	LS	ML	P value
D,×10^{-3} [mm^2/s]	1.88 ± 0.52	1.96 ± 0.48	0.00027*	1.48 ± 0.38	1.54 ± 0.36	0.0091*
K	0.79 ± 0.20	0.68 ± 0.21	<0.0001*	0.94 ± 0.20	0.81 ± 0.19	<0.0001*

Table 2. *Comparison of diffusion kurtosis-derived parameters (mean and standard deviation) values from regions of interest in peripheral zone tissue thought to be benign and found in prostate cancer measured using least squares (LS) estimation and maximum likelihood (ML) estimation. The asterisk indicates significance (Kruskal-Wallis test P-value<0.05).*

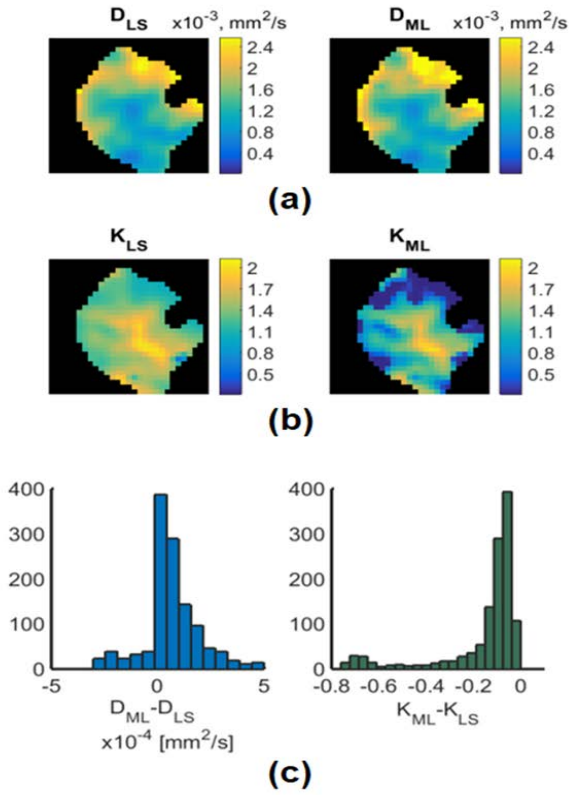

Figure 6. *Maps of (A) D, and (B) K obtained using LS and ML curve fitting from a region suspicious of cancer. (C) Histogram of DML-DLS and KML-KLS for voxels within this region. LS underestimated D and overestimated K.*

Discussion

Previous studies have shown that DKI is a promising approach in the assessment of PCa. A main limitation of DKI in body applications is low SNR even when phased array coils are used. When the LS estimation is used, low SNR results in bias in estimated parameters, which can limit the ability of the parameters to distinguish benign PZ from PCa. Here, the ML estimation is presented as an alternative to the standard LS algorithm for the analysis of DK data, which incorporates the noise model at higher noise levels thereby reducing the bias associated with DK parameter estimation. The simulation results demonstrated the impacts of low SNR on estimation of DK parameters. As the noise level increases, the bias in estimation of *D* and *K* increases when the LS estimator was applied. ML estimates of these parameters have lower bias in the SNR range of 5-25. Furthermore, the bias in the estimation of *DK* is substantially higher for PZ as compared with PCa. This is due to the higher diffusion values of PZ which results in more rapid signal attenuation as a function of b-value, and in turn results in greater sensitivity of *K* to SNR. The findings from computer simulations were confirmed by the results in the patient data.

The underestimation of *D* is dependent on both the SNR and the value of *D*. The bias for PZ (with higher D value) is greater than that for PCa. The overestimation of K also depends on the tissue diffusion coefficient. The values overestimated more substantially for PZ as compared with PCa. For high SNR, the noise distribution of the MR signal approached Gaussian distribution; hence, the differences for the estimated parameters from the two algorithms are minimal. Accounting for this noise-sensitive bias can result in more reliable estimates of *DK* parameters for PCa imaging.

Rosenkrantz et al. [7], investigated DK analysis for identification of PCa and, in distinguishing high- from low-grade cancer, found that DK analysis, as measured by *K*, showed significantly greater sensitivity in cancer detection as compared with ADC and *D*. Furthermore, *K* showed significantly greater accuracy in distinguishing high- from low-grade cancer as compared with ADC. Tamura et al. [9], obtained similar results to Rosenkrantz but whereas Rosenkrantz had used TRUS-guided biopsy as the standard of reference, Tamura's were based on radical prostatectomy specimens. To the best of our knowledge, this is the first study that explores the impact of low SNR in estimation of DKI parameters in the prostate using a ML approach. A similar study on the influence of noise correction on DKI in the brain found that noise correction had a strong impact on the estimation of parameters [16].

Recently, the use of phased array coil offered by vendors has increased substantially. For example, body and breast imaging are being performed with 32-channel phased array coils on 3T whole-body MR systems. Multi-channel coils can improve SNR, and, if sufficient, SNR can be obtained at 3-T, and prostate MR examinations, which include DW images, can be considered for routine clinical use without the endorectal coil. Although each coil element with a multiple coil system contributes only a small

amount of signal to the overall combined reconstructed image, the net contribution from all coil elements to generate sufficient SNR for clinical evaluation should be evaluated. The method we have presented is sufficiently general to address multi-channel coils. Specifically, following the method presented by Hardy et al. [18], and assuming no correlation between noise among phased array coil channels, the modified Rician PDF based on measured signal from multiple coils has been used. For the simulations and in vivo data *N*rec=8 was used.

To address the noise bias associated with the commonly used LS estimation the ML estimation has been selected. The ML approach is an unbiased estimator of Rician distribution data [4,5,9]. It has been shown that for the estimation of T2 relaxation [19,20], and diffusions parameters [4-6], the ML approach outperforms the more conventional methods such as LS.

Several other approaches have been evaluated in the literature to address this bias, including [21-25]. One approach is to incorporate the background noise into the signal intensity equation as was proposed by Jensen et al. [1], Kristoffersen et al. [23], compared various estimators of the diffusion coefficient for averaged and non-averaged noise. Based on Monte Carlo simulations, Kristoffersen showed that for averaged data, ML estimation performed similarly to the Md estimator, which is based on LS fitting of the measured signal to the Md value of the Rician distribution, and showed superior performance. There are no clear theoretical grounds for choosing an estimator [26], the ML approach provides a versatile approach to incorporating the noise from multiple receivers into the signal estimation and is generally considered the gold standard [6,23].

Accurate characterization of PCa can be achieved if the estimated parameters reflect the inherent intra-tumor heterogeneity such as variations in cell density, grade and structure. Because the ML estimate of K is unbiased to SNR and D, it provides a suitable approach to examine the underlying heterogeneous tumor microenvironment as shown by the evident heterogeneity in the K parameter maps (Figures 4-6). We intend to validate this observation with quantitative pathological information obtained from histopathological slides.

The present study has some limitations. First, the sources of the DK signal decay or alternative models to the DK model were not examined. A recent study in fresh and fixed prostate tissue ex vivo found that bi-exponential and DK models have similar information content for b-values up to 2000 s/mm^2 and beyond this b-value the bi-exponential model could be more appropriate. Another study suggested that the bi-exponential decay could be due to the compartmentalization of water by cell membranes [27]. The focus of this study was the DK model. Second, a total of nine b-values that were evenly spaced (above 800 s/mm^2) were used. Recent efforts by [28-30] have highlighted the focus on optimizing b-value for DKI. Third, the study consisted of a single radiologist who outlined the ROIs with knowledge of the location of cancerous sextants at biopsy but without reference to histopathological slides. To evaluate the clinical utility of the proposed estimation of DK parameters would necessitate correlation of tumor ROIs with whole-mount histopathology. Finally, it must be noted that the ML estimate of diffusion parameters is significantly limited if the noise level is not accurately known. When multi-channel phased array coils are used with a parallel imaging option, the noise level can be spatially varying [31]. Furthermore, other factors not accounted for by our approach, such as physiological noise, can also contribute to the noise. Although this simplified approach did not account for various contributions to noise or the spatial variability of noise, the results demonstrate the impact of the bias in *DK* parameter estimation when the SNR is low. In conclusion, by accounting for noise distribution, the ML analysis improves the accuracy of *DK* parameters, which can be beneficial when the SNR is low due to acquisition of higher b-values and can be utilized to acquire higher spatial resolution maps.

References

1. Jensen JH, Helpern JA, Ramani A, Lu H, Kaczynski K. Diffusional kurtosis imaging: the quantification of non-gaussian water diffusion by means of magnetic resonance imaging. *Magn Reson Med.* 2005; 53: 1432-1440.
2. Lu H, Jensen JH, Ramani A, Helpern JA. Three-dimensional characterization of non-gaussian water diffusion in humans using diffusion kurtosis imaging. *NMR Biomed.* 2006; 19(2):236-47.
3. Jensen JH, Helpern JA. MRI quantification of non-Gaussian water diffusion by kurtosis analysis. *NMR Biomed.* 2010; 23: 698-710.
4. Gudbjartsson H, Patz S. The Rician distribution of noisy MRI data. *Magn Reson Med*. 1995; 34: 910-914.
5. Sijbers J, den Dekker AJ, Scheunders P, Van Dyck D. Maximum-likelihood estimation of Rician distribution parameters. *IEEE Trans Med Imaging.* 1998; 17: 357-361.
6. Walker-Samuel S, Orton M, McPhail LD, Robinson SP. Robust estimation of the apparent diffusion coefficient (ADC) in heterogeneous solid tumors. *Magn Reson Med*. 2009; 62: 420-429.
7. Rosenkrantz AB, Sigmund EE, Johnson G, et al. Prostate cancer: feasibility and preliminary experience of a diffusional kurtosis model for detection and assessment of aggressiveness of peripheral zone cancer. *Radiology.* 2012; 264: 126-135.
8. Suo S, Chen X, Wu L, et al. Non-Gaussian water diffusion kurtosis imaging of prostate cancer. *Magn Reson Imaging.* 2014; 32: 421-427.
9. Tamura C, Shinmoto H, Soga S, et al. Diffusion kurtosis imaging study of prostate cancer: preliminary findings. *J Magn Reson Imaging.* 2014; 40: 723-729.
10. Quentin M, Pentang G, Schimmoller L, et al. Feasibility of diffusional kurtosis tensor imaging in prostate MRI for the assessment of prostate cancer: preliminary results. *Magn Reson Imaging*. 2014; 32: 880-885.
11. Roethke MC, Kuder TA, Kuru TH, et al. Evaluation of Diffusion Kurtosis Imaging Versus Standard Diffusion Imaging for Detection and Grading of Peripheral Zone Prostate Cancer. *Invest Radiol*. 2015; 50: 483-489.
12. Wiest-Daessle N, Prima S, Coupe P, Morrissey SP, Barillot C. Rician noise removal by non-Local Means filtering for low signal-to-noise ratio MRI: applications to DT-MRI. *Med Image Comput Comput Assist Interv.* 2008; 11: 171-179.
13. Dietrich O, Raya JG, Reeder SB, Ingrisch M, et al. Influence of multichannel combination, parallel imaging and other reconstruction techniques on MRI noise characteristics. *Magn Reson Imaging*. 2008; 26: 754-762.
14. Dietrich O, Raya JG, Reeder SB, Reiser MF, Schoenberg SO. Measurement of signal-to-noise ratios in MR images: influence of multichannel coils, parallel imaging, and reconstruction filters. *J Magn Reson Imaging.* 2007; 26: 375-385.
15. Coupe P, Manjon JV, Gedamu E, et al. Robust Rician noise estimation for MR images. *Med Image Anal.* 2010; 14: 483-493.
16. Andre ED, Grinberg F, Farrher E, et al. Influence of noise correction

on intra- and inter-subject variability of quantitative metrics in diffusion kurtosis imaging. *PloS one.* 2014; 9: e94531.
17. Constantinides CD, Atalar E, McVeigh ER. Signal-to-noise measurements in magnitude images from NMR phased arrays. *Magn Reson Imaging.* 1997; 38: 852-857.
18. Hardy PA, Andersen AH. Calculating T2 in images from a phased array receiver. *Magn Reson Imaging.* 2009; 61: 962-969.
19. Bonny JM, Zanca M, Boire JY, Veyre A. T2 maximum likelihood estimation from multiple spin-echo magnitude images. *Magn Reson Imaging.* 1996; 36: 287-293.
20. Karlsen OT, Verhagen R, Bovee WM. Parameter estimation from Rician-distributed data sets using a maximum likelihood estimator: application to T1 and perfusion measurements. *Magn Reson Imaging.* 1999; 41: 614-623.
21. Dietrich O, Heiland S, Sartor K. Noise correction for the exact determination of apparent diffusion coefficients at low SNR. *Magn Reson Imaging.* 2001; 45: 448-453.
22. Basu S, Fletcher T, Whitaker R. Rician noise removal in diffusion tensor MRI. *Med Image Comput Comput Assist Interv.* 2006; 9: 117-125.
23. Kristoffersen A. Optimal estimation of the diffusion coefficient from non-averaged and averaged noisy magnitude data. *J Magn Reson.* 2007; 187: 293-305.
24. Clarke RA, Scifo P, Rizzo G, et al. Noise correction on Rician distributed data for fibre orientation estimators. *IEEE Trans Med Imaging.* 2008; 27: 1242-1251.
25. Andersson JL. Maximum a posteriori estimation of diffusion tensor parameters using a Rician noise model: why, how and but. *Neuroimage.* 2008; 42: 1340-1356.
26. Tisdall MD, Atkins MS, Lockhart RA. Maximum likelihood estimators in magnetic resonance imaging. *Inf Process Med Imaging.* 2007; 20: 434-445.
27. Mulkern RV, Barnes AS, Haker SJ, et al. Biexponential characterization of prostate tissue water diffusion decay curves over an extended b-factor range. *Magn Reson Imaging.* 2006; 24: 563-568.
28. Poot DH, den Dekker AJ, Achten E, Verhoye M, Sijbers J. Optimal experimental design for diffusion kurtosis imaging. *IEEE Trans Med Imaging.* 2010; 29: 819-829.
29. Yan X, Zhou M, Ying L, et al. Evaluation of optimized b-value sampling schemas for diffusion kurtosis imaging with an application to stroke patient data. *Comput Med Imaging Graph.* 2013; 37: 272-280.
30. Hansen B, Jespersen SN. Data for evaluation of fast kurtosis strategies, b-value optimization and exploration of diffusion MRI contrast. *Sci Data.* 2016; 3: 160072.
31. Hutton C, Balteau E, Lutti A, Josephs O, Weiskopf N. Modelling temporal stability of EPI time series using magnitude images acquired with multi-channel receiver coils. *PloS one.* 2012; 7: e52075.

Correspondence: Yousef Mazaheri, Department of Medical Physics, Memorial Sloan Kettering Cancer Center, New York, NY, USA, Tel: 646-888-4520; E-mail: mazahery@mskcc.org

Rec: Jun 13, 2018; Acc: Jul 05, 2018; Pub: Jul 09, 2018

J Clin Med Imag. 2018;1(2):6
DOI: gsl.jcmi.2018.00006